Account of the diversity of tunneling spectra at the germanene/Al(1 1 1) interface

Davide Sciacca, Nemanja Peric, Maxime Berthe, Louis Biadala, Carmelo Pirri, Mickael Derivaz, Natalia Massara, Pascale Diener, B. Grandidier

Account of the diversity of tunneling spectra at the germanene/Al(111) interface

Davide Sciacca,[1] Nemanja Peric,[1] Maxime Berthe,[1] Louis Biadala,[1] Carmelo Pirri,[2] Mickael Derivaz,[2] Natalia Massara,[2] Pascale Diener,[1,*] and Bruno Grandidier[1]

[1] *Institut d'Electronique, de Microélectronique et de Nanotechnologie, UMR 8520, 59650 Villeneuve d'Ascq, France*
[2] *Institut de Science des Materiaux de Mulhouse IS2M UMR 7361 CNRS-Université de Haute Alsace, 3 bis rue Alfred Werner, 68057, Mulhouse, France*

Despite the wealth of tunneling spectroscopic studies performed on silicene and germanene, the observation of a well-defined Dirac cone in these materials remains elusive. Here, we study germanene grown on Al(111) at submonolayer coverages with low temperature scanning tunneling spectroscopy. We show that the tunnelling spectra between the Al(111) surface and germanene nanosheets are identical. They exhibit a clear metallic behaviour at the beginning of the experiments, that highlights the strong electronic coupling between the adlayer and the substrate. Over the course of the experiments, the spectra deviate from this initial behaviour, although consecutive spectra measured on the Al(111) surface and germanene nanosheets are still similar. This spectral diversity is explained by modifications of the tip apex, that arise from the erratic manipulation of the germanium adlayer. The origin of the characteristic features such as a wide band gap, coherence-like peaks or zero-bias anomalies are tentatively discussed in light of the physical properties of Ge and AlGe alloy clusters, that are likely to adsorb at the tip apex.

I. INTRODUCTION

Dirac cones in the band structure of graphene provides massless fermions, at the origin of outstanding physical properties such as the half-integer quantum hall effects, ultrahigh carrier mobility and minimum conductivity [1, 2]. Their existence can be readily determined with scanning tunnelling spectroscopy (STS), where the measurement of the differential conductance in the vicinity of the Fermi level is proportional to the density of states (DOS). For example, when graphene flakes are decoupled from a highly oriented pyrolytic graphite, a typical V-shaped DOS, vanishing at the Dirac point, signature of a Dirac cone, is usually measured with STS [3]. Similar to graphene, silicene and germanene should exhibit Dirac cones because of the honeycomb structure of their lattice [4, 5]. Nevertheless, the longer bond lengths in silicene and germanene yields a buckled structure, which slightly modifies their electronic structure. As the spin-orbit coupling increases with the degree of buckling, a small band gap has been predicted in addition to the linear energy dispersion [6]. So far, the presence of a small band gap has never been reported and only a few works have observed a differential conductance with a V-shape centred at the Fermi level [7–10]. Although the Dirac fermion nature of the charge carriers has still to be proved in these examples, where the spectra should develop into a sequence of Landau levels with a square root dependence on the magnetic field, the majority of the experimental works has nonetheless reported tunnelling spectra that differ from the V-shape characteristic in the region of the Fermi level [11–20]. This behaviour has been attributed to the strong electronic coupling between the silicene and germanene sheets with the host substrates. Moreover, a careful inspection of all the experimental spectra reported for a given system reveals significant deviations between the measured characteristics. For example, if we consider the (4x4) phase of silicene grown on the Ag(111) surface, Ref. [11] and [12] show differential conductance curves consisting of two symmetric branches increasing with bias at both polarities, whereas the curves displayed in Ref. [13], [14] and [15] have a clear asymmetric shape. Moreover, the Fermi level is inconsistently positioned close to the negative branch [11, 13] or to the positive branch [14, 15]. Also, some spectra are featureless around the Fermi level [11, 12, 16], while others show many peaks [14, 15, 17, 18]. Similar variations have been found for germanene grown on Pt/Ge(110) islands [7, 21, 22]. Different reasons were invoked to explain these variations, among them, the temperature of the measurements, spatial fluctuations of the electronic coupling between the sheet and the underlying substrate, and, the electronic structure of the tip used in scanning tunnelling microscopy (STM). Indeed, the local density of states (LDOS) of a silicene or gemanene sheet measured in tunnelling spectroscopy is always influenced by the bias-dependent transmission probability and the LDOS of the STM tip. Usually, the LDOS of a tungsten tip is considered as constant over a wide range of energy [23]. This flat LDOS tip leads to a differential conductance proportional to the LDOS of the sample. However many experiments have shown the key role of the tip LDOS in STS measurement [24–28].

* pascale.diener@isen.iemn.univ-lille1.fr

Here, we report STS measurements performed on the (3x3) phase of germanene grown on the Al(111) surface [20, 29, 30]. Comparison of the tunnelling spectra with the ones obtained on clean Al islands reveals a similar metallic behaviour, when the measurements are performed with fresh and clean STM tips. As the tips are used, the spectra are found to deviate from this initial behaviour, although they still show a very good similarity between the germanene and Al islands. Some spectra show a V-shape, that are also observed on the surrounding Al islands, whereas other spectra depart from this characteristic. We explain the variability of the spectral features by the fortuitous manipulation of the surface during the course of the experiments. Germanene nanosheets can be scraped, resulting in the formation of clusters on the surface or in the deposition of new germanene islands. While these spurious modifications of the germanene adlayer show the weak mechanical coupling between the germanene nanosheet and the Al(111) surface, they also involve a contamination of the STM tips by Ge and Al atoms. Based on the electronic structures of numerous Ge and AlGe alloy clusters, that have been predicted in the literature, we speculate on the origin of the broad spectral diversity observed when the germanene/Al(111) interface is characterized with STS.

II. EXPERIMENT

Sample preparation and experiments were carried out in an ultrahigh vacuum chamber (UHV) with a base pressure lower than 5 x 10^{-11} Torr. Germanene was synthesized following the recipe of Derivaz et al. [29]: clean and well-ordered Al(111) surfaces were first prepared by Ne bombardment (800V, 5 x 10^{-6} Torr) and subsequent annealing at 450°C for 1 hour; then atomic Ge was evaporated from a Ge(001) crystal onto the clean and well-ordered Al(111) surface heated at a temperature between 80 and 100 °C. The deposited film was then characterized with an Omicron low-temperature scanning tunnelling microscope (LT-STM) at liquid nitrogen (77K) and liquid helium (5K) temperatures. Atomically sharp tips were obtained via chemical etching of a tungsten wire in NaOH solution. The wires were thoroughly heated in UHV to obtain clean tips, the final cleaning step involving a cycle of flashes with a duration of 10s at temperatures higher than 2000 K, to ensure a high purity of the tungsten material at the apex [31, 32]. Such flashes were also repeated in the course of the STM experiments to get rid of the adsorbed species and recover an apex free of contaminants. Typical STM imaging conditions with these tips were obtained for sample bias ranging between -2.0 and 2.0V and with tunnelling set-point currents smaller than 400 pA.

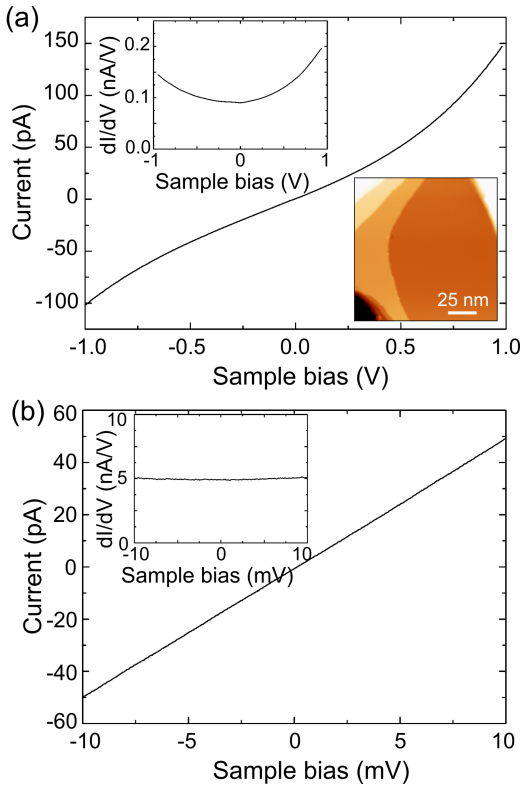

FIG. 1. I-V curves and the related dI/dV spectra (upper insets) measured on the clean Al(111) for feedback conditions of (a) V=-1.0V, I=100pA,and (b) V=-10 mV, I=50pA. Lower inset: STM image of the clean Al(111) surface acquired at a temperature of 5 K.

STS measurements were performed by recording both I(V) curves and the analog derivative dI/dV curves with a Signal Recovery lock-in amplifier, using a modulating frequency of 480 Hz, a variable modulating amplitude between 1 and 7 mV RMS and a variable RC time constant between 10 and 20 ms. Prior to the STM experiments with the germanene sample, the tips were tested on a clean Al(111) surface to make sure that the tunnelling spectra were featureless between -1 and +1 V and in particular around the Fermi level. As shown in Figure 1, the absence of any features in the I(V) and dI(V)/dV curves is consistent with a constant LDOS for the tip apex. The acquisition of local spectra measured at constant tip-sample separation can also be extended to a grid of pixel in a STM image. The method, denoted Current Imaging Tunneling Spectroscopy (CITS), was performed by acquiring a 64x64 grid of spectra simultaneously with the STM images consisting of a grid of 256x256 pixels. Between the measurements of two consecutive spectra, a constant stabilization voltage was applied to the sample and the feedback loop was active, so that the tip height was adjusted to maintain a constant tunnelling current and safely moved to the next pixel.

III. RESULTS

Figure 2 shows a large scale STM image obtained for a full coverage of the Al(111) surface with germanium. Multiple terraces are visible. They are separated with a step height of 2.3 Å, which compares well with the Al(111) step height. All the terraces are covered with the same periodic array of bright protrusions showing a hexagonal symmetry. The distance between two neighbouring protrusions is 8.7±0.2Å. The observed structure is compatible with the previously reported 3x3 reconstruction of germanene compared to the periodicity of the Al(111) lattice [20, 30, 33]. In this configuration, previous theoretical calculations showed that the protrusions correspond to a Ge atom that is uplifted by $1.5 \sim 2.1$ Å compared to the other atoms in the unit cell, producing a hexagonal lattice in the STM image [30, 33]. We also note the presence of a few Y-shape structures characterized by three bright protrusions and a fourth one in the hollow site between the three top Ge atoms (two of these Y-shape structures are highlighted by dashed circles in figure 2). For this sample, the concentration of the Y-shape defects was 9 x 10^{11} cm^{-2}. Finally, bright clusters are seen here and there, that we attribute to the slight extra amount of germanium adsorbed on the surface.

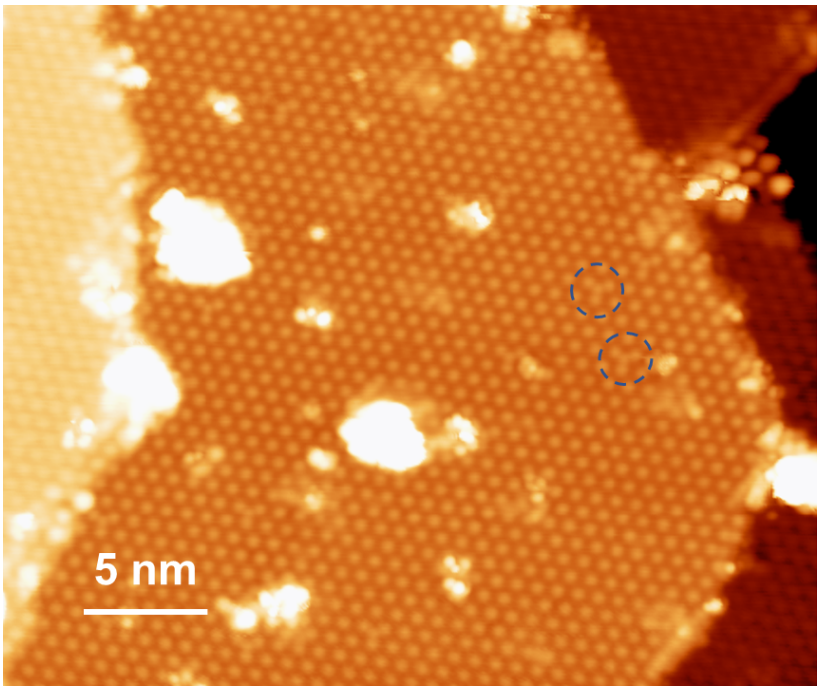

FIG. 2. Large scale filled-state STM image of monolayer germanene on Al(111). Typical Y-shape defects are shown in dashed circles. Image parameters: sample bias V= -1V, current I=50pA, temperature T=77K.

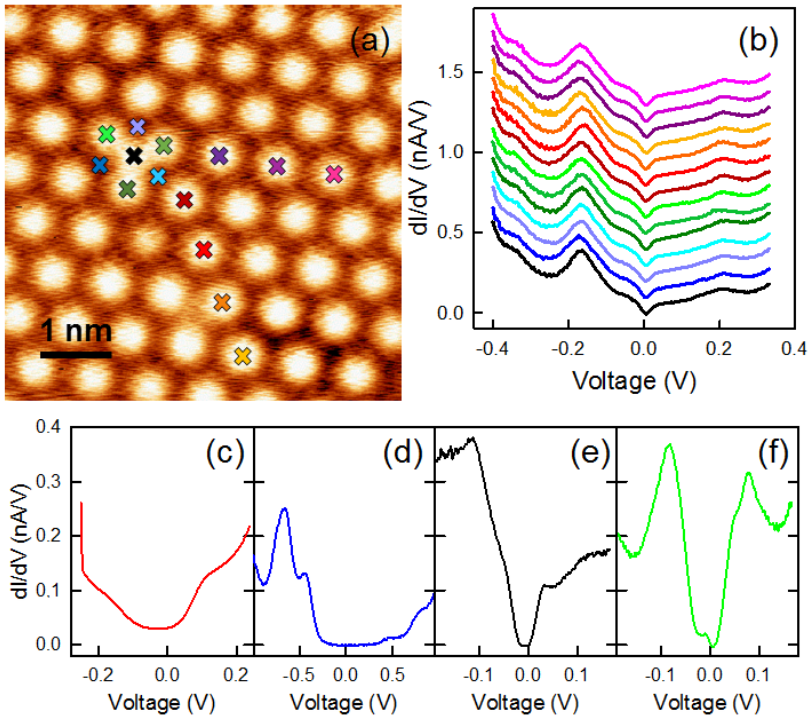

FIG. 3. (a) Spatially-resolved tunneling spectra of a germanene area with an Y-shape defect, V=-0.4V, I=100pA, T=5K. (b) Different spectra acquired at the location highlighted in (a). (c-f) Different dI/dV acquired on monolayer 3x3 germanene on Al(111), measured at different temperatures with different setpoint bias and currents. (c) 77K, -0.25V, 100pA. (d) 77K, -0.75V, 100pA. (e) 5K, -0.2V, 90pA. (f) 5K, -0.2V, 60pA.

STS measurements were performed on this surface, with particular attention to the spatial dependence of the I(V) characteristics. Figure 3(a) shows spatially resolved tunnelling spectra on an area which includes a Y-shaped defect. A sequence of twelve dI/dV spectra selected either on the top Ge atoms, in the hollow sites or on the Y-shaped defect are displayed in Figure 3(b). Remarkably, they all show the same characteristics with two peaks at -0.18V and +0.20V and a small dip at zero bias, corresponding to the Fermi level position in the sample. The position of the peaks and the minimum at the Fermi level are not affected by the local environment. Although the spectra show a high spatial reproducibility, we have found that subsequent tunneling measurements performed on similar clean and well-ordered areas with the same tip over the course of the experiments do not exhibit the same spectral features. Figure 3(c-f) show a representative set of differential conductance measurements. In spectrum (c), the differential conductance has a finite value when the bias approaches zero, indicating a metallic behaviour. Conversely, in spectrum (d), the differential conductance exhibits a zero-conductance gap about 500mV around the Fermi level. Much smaller zero-conductance gaps are also found such as the one visible in Figure 3(e), with a width of 35 meV. Significant variations also exist in the number and shape of the measured peaks and plateau, Figure 3(f) exhibiting coherence peaks-like around the Fermi level, for example.

Due the large variety of spectra encountered on the germanene surface, it is important to make sure that the LDOS of the STM tip is constant over a wide range of energy prior to the interpretation of the spectral features. As a result, samples with sub- monolayer coverage were also grown, so that bare Al areas can be probed to provide reference spectra. Figure 4 shows an example of a germanene nanosheet, that grew on an Al(111) terrace. The 3x3 reconstruction is still observed, with interatomic distances and step heights that match the ones measured at monolayer coverage. Based on the height profile shown in Figure 4, the average height of the island appears at the same level as the rest of the Al terrace, the top Ge atoms protruding 0.30 Å above this mean level for the best tip conditions. While small defective areas decorated possibly with Ge atoms and clusters are also seen in the STM image, a large part of the Al terrace is unaffected by the growth, allowing to acquire reference tunnelling spectra.

Measurements shown in Figure 5 were obtained with a fresh and clean STM tip at a temperature of 5K. In the reduced range of bias between -0.1 V and +0.1 V, the I(V) curves measured on the bare Al surface are all linear whatever the set-point current is. This behaviour is also found on a larger bias range, extending from -1.0 V to +1.0 V. It is consistent with the spectra obtained on the clean Al(111) surface in Figure 1 and agrees with the metallic nature of the substrate and the tip. It indicates that the contribution of any surface states of the Al surface is negligible,

in particular those positioned at the K point, 0.7 eV below the Fermi level in the band gap of the three-dimensional Al band structure projected onto the two-dimensional Brillouin zone [34]. Indeed, these states having a high parallel wave-vector should strongly decay into vacuum, implying a small transmission probability. Therefore, the linear characteristic found on an Al(111) terrace shows that the LDOS of the STM tip can be considered constant over the whole energy range. Reference spectra being established, the same tip was used to probe the germanene island located nearby, as pointed out in the STM image of Figure 5. Again, I(V) were recorded with different set-point currents to assess any influence of the tip-sample distance as the tip becomes closer to the surface with increasing currents. Remarkably, all I(V) curves measured on the germanene island match the I(V) curves measured on the Al(111) surface, These measurements show a clear metallic behaviour, which highlights the strong electronic coupling between germanene and aluminium, preventing the formation of a small band gap in germanene.

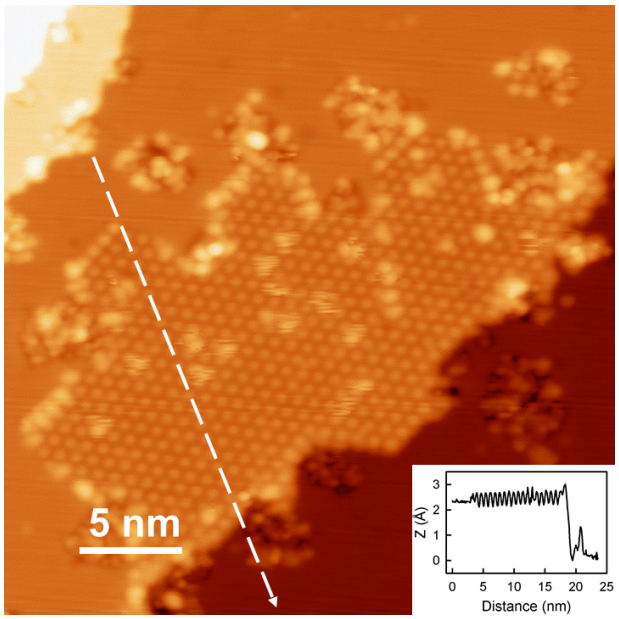

FIG. 4. STM image of submonolayer germanene growth on Al(111). V=-1.5V, I=50pA. T=77K. Inset: Height profile measured across the germanene island along the dashed line.

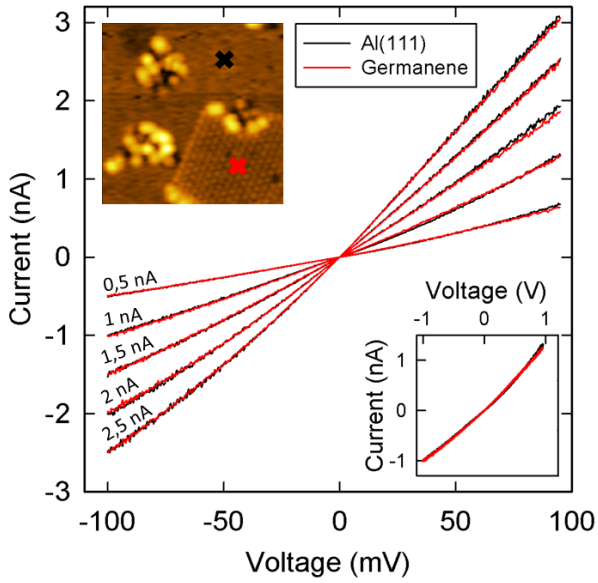

FIG. 5. I-V curve measured as a function of setpoint current on Al(111) and germanene areas indicated by crosses in the STM image of the upper inset at 5K. Inset: similar I(V) curves measured on a wider bias range with a setpoint current of 1 nA.

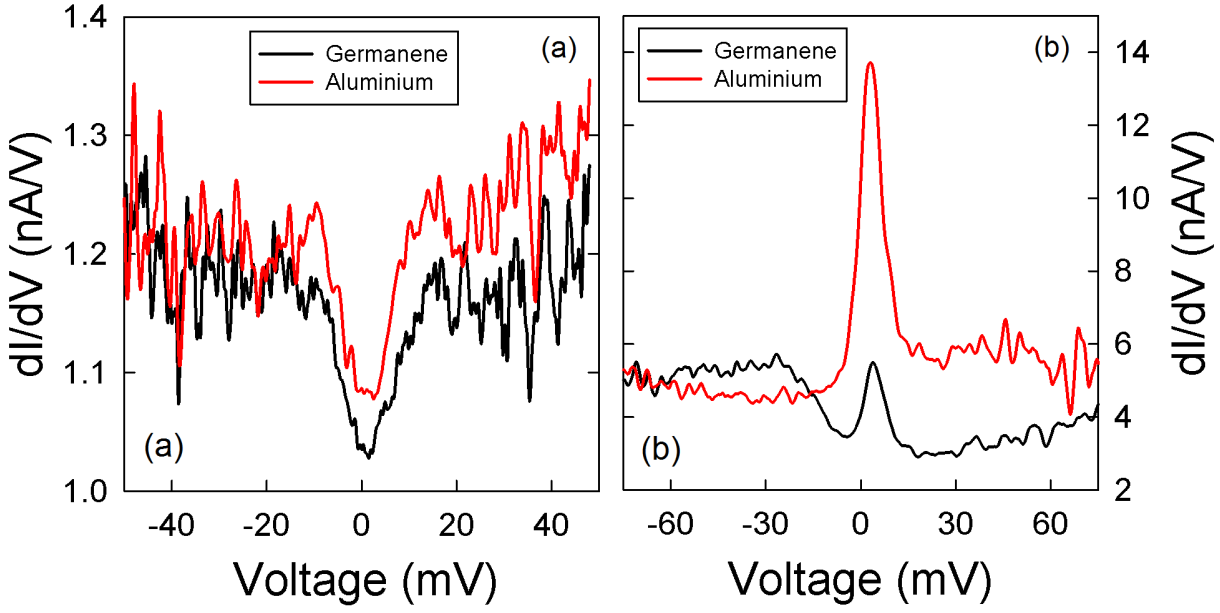

FIG. 6. Two different example of dI/dV spectra measured on Al(111) and germanene of non-trivial interpretation. Both couple of spectra have been acquired at 5K, (a) V=-0.5V, I=60pA, (b) V=-0.1V, 500pA.

During the run of the experiments with the same tip, the acquisition of the additional spectra in other areas confirmed the similarity of the spectra acquired on the bare Al(111) surface and the germanene islands. However, the shape of the spectra was different from the initial linear behaviour. Two examples are shown in Figure 6. In Figure 6(a), a dip, that could be approximated with a V-shape-like function, is clearly seen in the differential conductance of both entities. Since this feature centred at the Fermi level is not expected for the Al(111) surface, we dismiss its origin to be related to the existence of a Dirac cone in the germanene nanosheet. Alternatively, Figure 6(b) exhibits a strong peak, which is slightly shifted by 3.5 mV above the Fermi level. Again, the STS measurements between the Al surface and the germanene islands show the same peak, albeit to a modification of the peak intensity. As such a peak is not expected for the Al(111) surface, we rule out it to be caused by the electronic structure of the germanene nanosheet. Therefore, the diversity of the spectra obtained as the tip becomes used points to its crucial contribution to produce the spectral features visible in Figures 3 and 6. These change of behaviors with time suggests that the tip gets contaminated as it probes the sample.

So far, in the literature has been shown that the STM tip can induce a change of the germanene structure at room temperature, switching between a honeycomb lattice to a hexagonal lattice [33]. However, we have encountered more dramatic events at low temperatures. As shown in Figure 7, a germanene island can be disrupted when the tip is scanning on top of the nanosheet. The lower part of the island visible in Figure 7(a), that exhibits a typical 3x3 reconstruction and the characteristic step height (see Figure 7(b)), has disappeared in Figure 7(c), leaving behind a large cluster with a height of 2.1 nm at the bottom right of the island. At the place of the island, the bare Al surface is partially recovered, but sparsely decorated with small clusters. Moreover, a narrow crack appears in the surface, as shown in Figure 7(d), and its existence suggests that some Al atoms have been stripped off during the manipulation of the Ge adlayer. While most of the Ge and Al atoms, that were removed, have certainly been incorporated in the clusters seen on the surface, we cannot rule out the adsorption of atoms and clusters on the tip apex also. Figure 8 reveals another example of the surface modification under scanning conditions. The topographic and current images in Figures 8(a) and (b) show an isolated germanene island. Upon the measurement of an I(V) curve with a close feedback loop in the top left part of the STM image, a germanene island appears in Figure 8(c) and (d). During the next scans with constant feedback conditions, the surface is found to evolve to the final arrangement of the terraces seen in Figure 8(e) and (f). Surprinsigly, some new terraces show the 3x3 structure of germanene, meaning that nanosheets have been redeposited or displaced under the action of the STM tip. Although the occurrence of such events is the exception rather than the rule, they emphasize on the fragility of the germanene adlayer. This is consistent with the weak adsorption energy calculated for Ge atoms on the Al(111) surface [33, 35].

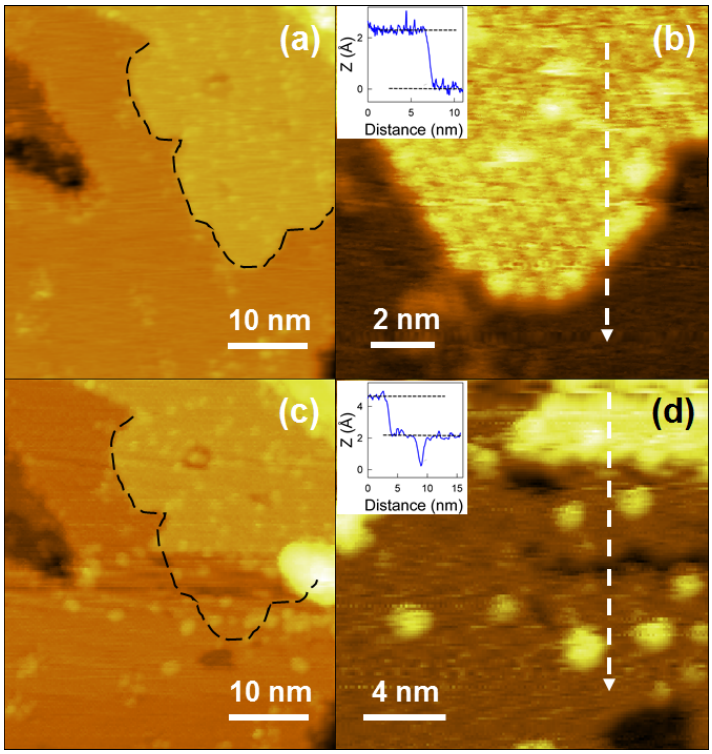

FIG. 7. (a) Initial STM topography of a germanene island. (b) Atomically resolved image of the lower edge of germanene island, showing the typical 3x3 structure. Inset: Height profile across the germanene island along the dashed line. (c) STM topography of the island after its unintentional manipulation. (d) Zoom on the removed area, with height profile in the inset. All the images were acquired at 77K, V=-1V, I=50pA.

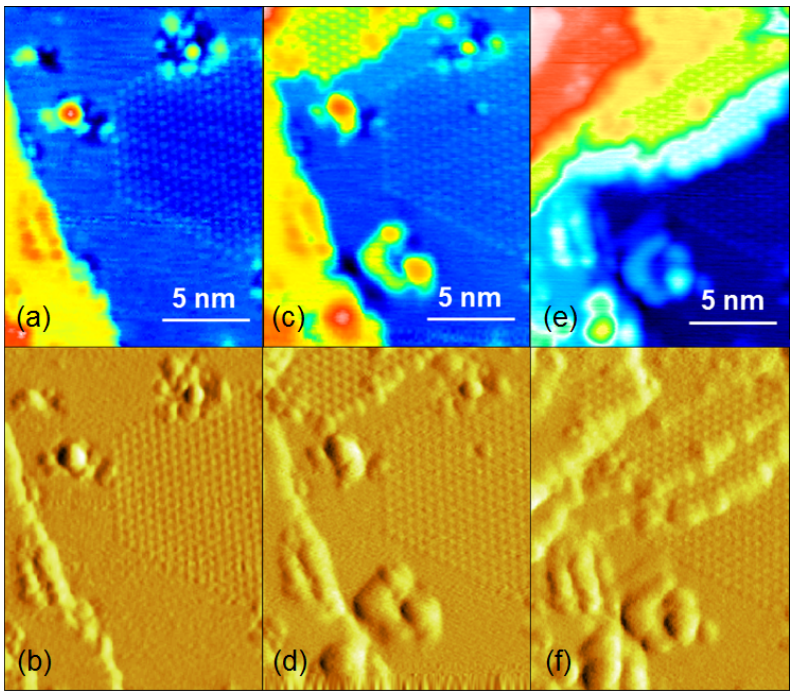

FIG. 8. Sequence of STM images showing the real time appearance of germanene island. (a) Initial configuration of a hexagonal germanene island, with the related current image (b). (c) and (d) Modified configuration. The new terrace is a monolayer germanene step as shown in (d). (e-f) Final equilibrium position, with a bilayer+monolayer. All the images have been acquired at 77K, V=-1V, I=5pA.

As an additional hint for the key role of adsorbed species at the tip apex in STS, we show CITS result in Figure 9. The high resolution STM image of the 3x3 reconstruction of germanene simultaneously acquired with the grid of I(V) and dI(V)/dV curves, reveals sequences of topographic lines with a high density of glitches. Two types of regions exist, one with a low level of noise and one with a higher level of noise. The analysis of the spectra reveals the existence of two sets of spectra, consistent with the absence or presence of noise in the STM image. The lower spectrum in Figure 9(b) shows a peak at negative bias and an apparent band gap of 50 mV, that extends more above the Fermi level. The upper spectrum of Figure 9(b) resembles the lower one, but the peak is shifted towards the Fermi level and the apparent band gap is almost closed. The change of the image quality is therefore correlated with the change observed in the differential conductance. At a bias of -20 mV, which corresponds to the bias of the peak seen in the lower spectrum, the differential conductance is the highest in the topographic areas free of glitches (Figure 9c)). Such a correlation is emphasized when a line of spectra is plotted along the dashed line indicated in the STM image (Figure 9(d)). As the area probed by the tip is clean and well-ordered, such measurements demonstrate the STM tip is at the origin of these sudden but repeatable changes in the tunnelling spectra. Based on these three examples, we believe that, despite the low temperature of the experiments, the STM tip can be easily contaminated by single atoms or clusters of Ge or/and Al atoms, resulting in characteristics with complex shapes.

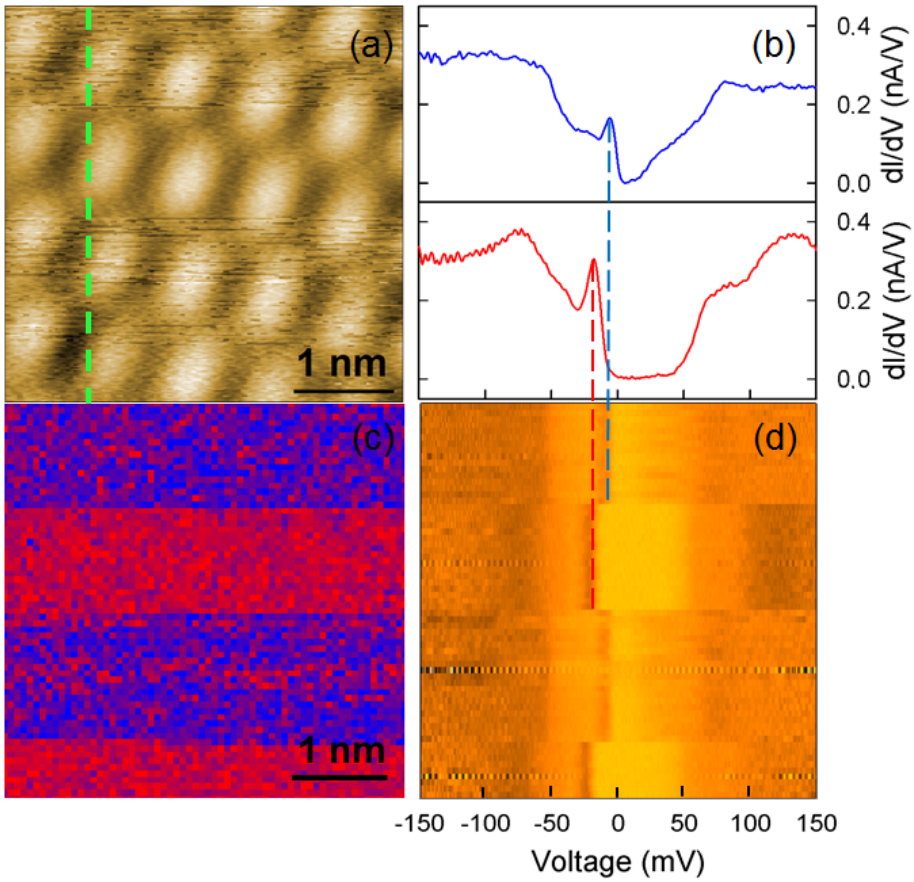

FIG. 9. (a) Topography of a defect-free germanene area, V=-0.15V, I=50pA, T=5K. (b) The two classes of spectra measured during the CITS. (c) Differential conductance map, measured at -20mV, blue and red as in (b). (d) Strips view representation of the 64 spectra along the green line in (a).

IV. DISCUSSION

The similarity of the spectra measured on the bare Al(111) islands and on the germanene nanosheets indicates a tunnelling current dominated by the band structure of the Al crystal close to the Fermi level. We attribute this effect to the significant charge transfer calculated between the Ge atoms in contact with the Al(111) surface [30, 36], that certainly keeps the transmission probability high across the tunnelling junction. However, with continuous scanning of the surface over time, the spectra deviate from this linear behaviour around the Fermi level and show apparent

gaps and peaks. We attribute the presence of these features to the formation of a nonconstant tip LDOS. Although the existence of tips with a nonuniform density of states has been reported in the literature [24–28], we note that the probability to get such a tip is rather high with a germanene sample. Due to the weak bonding of the Ge adlayer that arises from the jellium-like character of the electron distribution at the Al(111) surface [29], the germanene nanosheets can easily lose atoms or clusters, that adsorb on the tip apex resulting in nonconstant tip LDOS. Opposite to graphene, where small flakes have been displaced on a surface without any alteration [37, 38], we have always failed in controlling the manipulation of a germanene nanosheet to slide on the Al(111) surface. Manipulation have always led to a drastic transformation of the sheet, causing either the formation of clusters on the surface (Figure 7) or the reshaping of the terraces to produce new germanene islands (Figure 8). This observation is in agreement with the difficulty to maintain Ge atoms in a plane, as observed with high-resolution transmission electron microscopy where two-dimensional Ge clusters have been found to morph into stable three dimensional clusters [39].

Based on the different apex termination that are likely to occur, we can speculate on their impact on the tunnelling spectra. For example, the weak attachment of a small Ge crystallite at the end of the tip could give rise to a double tunneling junction structure, where electrons would be transferred through the states of the nanocrystals. As a result, the tunnelling spectra exhibit a zero conductance gap, which is caused by the band gap of the nanocrystal. This configuration accounts for the spectra with the largest apparent band gap, like the one seen in Figure 3(d), the width of the band gap being consistent with the one reported in the literature for Ge nanocrystals [40]. Smaller Ge crystallites can also exist. In particular, a wide range of Ge clusters have been predicted to exist [41]. Depending on the Ge cluster size, theoretical calculations of the separation between the highest occupied and lowest unoccupied molecular orbitals yield value in the range of the apparent band gap found by the STS measurements [42, 43]. Instead of crystallites, amorphous Ge clusters could also self-assemble at the tip apex. They might have a density of states that can be relatively high in the vicinity of the Fermi level. Tunnelling through such a quasi-metallic cluster also results in an apparent band gap in the spectra due to electron-electron interaction. This Coulomb gap was estimated by Efros [44] and can explain the observation of spectra with small apparent band gap of a few mV to tens of mV, as the ones seen in Figures 3(e) and (f). Similar behaviour should arise when Ge clusters are doped with W atoms of the tip or Al atoms of the surface [45, 46]. Missing areas of the Al surface were observed after the manipulation of the germanene islands (Figure 7(d)), suggesting that Ge clusters containing Al atoms could exist at the tip apex. In this case, the observation of a Fano resonance is possible, similar to the peak seen in Figure 6(b), since interference effects between direct tunnelling from the tip to the surface and tunnelling through the energy level of the Al impurity might occur [47]. Clusters with different stoichiometry may exist and we could even imagine to stabilize Al-rich clusters. Depending on the number of Al atoms, it has been shown that some clusters become more stable with a magic number of Al and Ge atoms. A typical example is Al icosahedral clusters consisting of 13 atoms, whose stability increases by substituting an Al atom with a Ge atom [48]. If weakly bound to the tip, such a cluster, could give rise to an apparent band gap in the tunnelling spectra [49]. It is interesting to note that mixture of Al and Ge films were found to show an enhanced superconductivity [50, 51], above the critical temperature of Al. Thus, we cannot rule out that these clusters show similar properties. The existence of superconducting clusters at the end of the tip could account for a vanishing DOS at the Fermi level or the observation of coherence peaks-like, similar to the spectra observed in Figures 3(f) and 6(a). Finally, as mentioned above, examination of Ge clusters with transmission electron microscopy have revealed the transformation of the clusters under the electron beam. These transformations can reach different equilibrium geometries or even lead to the fragmentation of the clusters with time, causing the appearance of different features in the tunnelling spectra. They could also explain the glitches observed in Figure 9 [39].

V. CONCLUSION

In summary, we have performed intensive tunnelling spectroscopic measurements of the germanene surface, taking care of comparing the spectra with reference spectra obtained on the bare Al(111) surface. When clean STM tips are used, a linear behaviour of the I(V) characteristics is found and indicates a metallic surface. However, as the tips become used, significant changes in the shape of the spectra occur, even though the spectra are spatially and temporally reproducible over a few hours. We attribute these changes to the weak bonding of the germanene layer with the Al(111) surface and the ease for the tip to capture Ge, Al or Ge-Al clusters. The vast zoology of these clusters explains the diversity of the spectra observed during the experiments. Our results highlight the instability of the germanene sheet when it loses contact with the Al substrate underneath, consistent with the lack of two-dimensional Ge crystallites in the gas phase. While they call for a greater care in the interpretation of tunnelling spectra acquired on fragile two-dimensional atomic crystals that do not exist in nature, they also bespeak the unforeseen richness of the electronic structure of Ge and Al clusters.

ACKNOWLEDGMENTS

This study was financially supported by the French National Research Agency (Germanene project ANR-17-CE09-0021-03), the EQUIPEX program Excelsior (Grant No. ANR-11-EQPX-0015) and the RENATECH network.

[1] K. S. Novoselov, A. K. Geim, S. Morozov, D. Jiang, M. Katsnelson, I. Grigorieva, S. Dubonos, Firsov, and AA, Nature **438**, 197 (2005).
[2] Y. Zhang, Y.-W. Tan, H. L. Stormer, and P. Kim, Nature **438**, 201 (2005).
[3] G. Li, A. Luican, and E. Y. Andrei, Phys. Rev. Lett. **102**, 176804 (2009).
[4] A. Acun, L. Zhang, P. Bampoulis, M. Farmanbar, A. van Houselt, A. Rudenko, M. Lingenfelder, G. Brocks, B. Poelsema, M. Katsnelson, *et al.*, J. Phys. Condens. Mat. **27**, 443002 (2015).
[5] S. Cahangirov, M. Topsakal, E. Aktürk, H. Şahin, and S. Ciraci, Phys. Rev. Lett. **102**, 236804 (2009).
[6] C.-C. Liu, W. Feng, and Y. Yao, Phys. Rev. Lett. **107**, 076802 (2011).
[7] C. Walhout, A. Acun, L. Zhang, M. Ezawa, and H. J. Zandvliet, J. Phys. Condens. Mat. **28**, 284006 (2016).
[8] L. Zhang, P. Bampoulis, A. Rudenko, Q. v. Yao, A. Van Houselt, B. Poelsema, M. Katsnelson, and H. Zandvliet, Phys. Rev. Lett. **116**, 256804 (2016).
[9] Z. Qin, J. Pan, S. Lu, Y. Shao, Y. Wang, S. Du, H.-J. Gao, and G. Cao, Adv. Mat. **29**, 1606046 (2017).
[10] J. Zhuang, C. Liu, Z. Zhou, G. Casillas, H. Feng, X. Xu, J. Wang, W. Hao, X. Wang, S. X. Dou, *et al.*, Adv. Sci. **5**, 1800207 (2018).
[11] D. Chiappe, C. Grazianetti, G. Tallarida, M. Fanciulli, and A. Molle, Adv. Mater. **24**, 5088 (2012).
[12] Y. Du, J. Zhuang, H. Liu, X. Xu, S. Eilers, K. Wu, P. Cheng, J. Zhao, X. Pi, K. W. See, *et al.*, ACS Nano **8**, 10019 (2014).
[13] B. Feng, Z. Ding, S. Meng, Y. Yao, X. He, P. Cheng, L. Chen, and K. Wu, Nano Lett. **12**, 3507 (2012).
[14] A. D. Álvarez, T. Zhu, J. Nys, M. Berthe, M. Empis, J. Schreiber, B. Grandidier, and T. Xu, Surf. Sci. **653**, 92 (2016).
[15] C.-L. Lin, R. Arafune, M. Kawai, and N. Takagi, Chin. Phys. B **24**, 087307 (2015).
[16] C. Grazianetti, D. Chiappe, E. Cinquanta, G. Tallarida, M. Fanciulli, and A. Molle, Appl. Surf. Sci. **291**, 109 (2014).
[17] C.-L. Lin, R. Arafune, K. Kawahara, M. Kanno, N. Tsukahara, E. Minamitani, Y. Kim, M. Kawai, and N. Takagi, Phys. Rev. Lett. **110**, 076801 (2013).
[18] P. De Padova, H. Feng, J. Zhuang, Z. Li, A. Generosi, B. Paci, C. Ottaviani, C. Quaresima, B. Olivieri, M. Krawiec, *et al.*, J. Phys. Chem. C **121**, 27182 (2017).
[19] C. Volders, E. Monazami, G. Ramalingam, and P. Reinke, Nano Lett. **17**, 299 (2016).
[20] S. Endo, O. Kubo, N. Nakashima, S. Iwaguma, R. Yamamoto, Y. Kamakura, H. Tabata, and M. Katayama, Appl. Phys. Expr. **11**, 015502 (2017).
[21] P. Bampoulis, L. Zhang, A. Safaei, R. van Gastel, B. Poelsema, and H. J. W. Zandvliet, J. Phys. Condens. Mat. **26**, 442001 (2014).
[22] L. Zhang, P. Bampoulis, A. van Houselt, and H. J. Zandvliet, Appl. Phys. Lett. **107**, 111605 (2015).
[23] J. A. Stroscio, R. Feenstra, and A. Fein, Phys. Rev. Lett. **57**, 2579 (1986).
[24] T. Klitsner, R. Becker, and J. Vickers, Phys. Rev. B **41**, 3837 (1990).
[25] J. Pelz, Phys. Rev. B **43**, 6746 (1991).
[26] R. Dombrowski, C. Steinebach, C. Wittneven, M. Morgenstern, and R. Wiesendanger, Phys. Rev. B **59**, 8043 (1999).
[27] M. Passoni, F. Donati, A. L. Bassi, C. S. Casari, and C. E. Bottani, Phys. Rev. B **79**, 045404 (2009).
[28] T. Kwapiński and M. Jałochowski, Surf. Sci. **604**, 1752 (2010).
[29] M. Derivaz, D. Dentel, R. Stephan, M.-C. Hanf, A. Mehdaoui, P. Sonnet, and C. Pirri, Nano Lett. **15**, 2510 (2015).
[30] W. Wang and R. I. Uhrberg, Beilstein J. Nanotech. **8**, 1946 (2017).
[31] O. Albrektsen, H. Salemink, K. Mo/rch, and A. Thölen, JVST B **12**, 3187 (1994).
[32] Z. Yu, C. M. Wang, Y. Du, S. Thevuthasan, and I. Lyubinetsky, Ultramicroscopy **108**, 873 (2008).
[33] R. Stephan, M. Derivaz, M.-C. Hanf, D. Dentel, N. Massara, A. Mehdaoui, P. Sonnet, and C. Pirri, J. Phys. Chem. Lett. **8**, 4587 (2017).
[34] S. Kevan, N. Stoffel, and N. Smith, Phys. Rev. B **31**, 1788 (1985).
[35] N. Gao, H. Liu, S. Zhou, Y. Bai, and J. Zhao, J. Phys. Chem. C **121**, 5123 (2017).
[36] R. Stephan, M. Hanf, M. Derivaz, D. Dentel, M. Asensio, J. Avila, A. Mehdaoui, P. Sonnet, and C. Pirri, J. Phys. Chem. C **120**, 1580 (2016).
[37] S. Kawai, A. Benassi, E. Gnecco, H. Söde, R. Pawlak, X. Feng, K. Müllen, D. Passerone, C. A. Pignedoli, P. Ruffieux, *et al.*, Science **351**, 957 (2016).
[38] X. Feng, S. Kwon, J. Y. Park, and M. Salmeron, ACS Nano **7**, 1718 (2013).
[39] S. Bals, S. Van Aert, C. Romero, K. Lauwaet, M. J. Van Bael, B. Schoeters, B. Partoens, E. Yücelen, P. Lievens, and G. Van Tendeloo, Nat. Commun. **3**, 897 (2012).
[40] Y. Nakamura, K. Watanabe, Y. Fukuzawa, and M. Ichikawa, Appl. Phys. Lett. **87**, 133119 (2005).
[41] W.-C. Lu, C. Wang, L.-Z. Zhao, W. Zhang, W. Qin, and K. Ho, Phys. Chem. Chem. Phys. **12**, 8551 (2010).
[42] Y. Negishi, H. Kawamata, F. Hayakawa, A. Nakajima, and K. Kaya, Chem. Phys. Lett. **294**, 370 (1998).
[43] J. Wang, G. Wang, and J. Zhao, Phys. Rev. B **64**, 205411 (2001).

[44] A. Efros and B. I. Shklovskii, J. Phys. C: Solid State Phys **8**, L49 (1975).
[45] J. Wang and J.-G. Han, J. Phys. Chem. A **110**, 12670 (2006).
[46] I. Chambouleyron and D. Comedi, J. Non Cryst. Solids **227**, 411 (1998).
[47] V. N. Mantsevich and N. S. Maslova, JETP Lett. **91**, 139 (2010).
[48] X. Gong and V. Kumar, Phys. Rev. Lett. **70**, 2078 (1993).
[49] X. Li and L.-S. Wang, Phys. Rev. B **65**, 153404 (2002).
[50] J. Hauser, Phys. Rev. B **3**, 1611 (1971).
[51] A. Fontaine and F. Meunier, Z. Phys. B Condens. Matter **14**, 119 (1972).